BJR

Received: 16 December 2015 | Revised: 16 January 2016 | Accepted: 20 January 2016

doi: 10.1259/bjr.20151055

Cite this article as:
Widmann G, Bischel A, Stratis A, Kakar A, Bosmans H, Jacobs R, et al. Ultralow dose dentomaxillofacial CT imaging and iterative reconstruction techniques: variability of Hounsfield units and contrast-to-noise ratio. *Br J Radiol* 2016; **89**: 20151055.

FULL PAPER

Ultralow dose dentomaxillofacial CT imaging and iterative reconstruction techniques: variability of Hounsfield units and contrast-to-noise ratio

[1]GERLIG WIDMANN, MD, [2]ALEXANDER BISCHEL, [3]ANDREAS STRATIS, MSc, [3]APOORV KAKAR, [3]HILDE BOSMANS, PhD, [3]REINHILDE JACOBS, PhD, [1]EVA-MARIA GASSNER, MD, [2]WOLFGANG PUELACHER, MD, DDS and [3,4]RUBEN PAUWELS, PhD

[1]Department of Radiology, Innsbruck Medical University, Innsbruck, Austria
[2]Department of Craniomaxillofacial Surgery, Innsbruck Medical University, Innsbruck, Austria
[3]OMFS-IMPATH Research Group, Department of Imaging & Pathology, University Leuven and Department of Oral and Maxillofacial Surgery, University Hospitals Leuven, Leuven, Belgium
[4]Department of Radiology, Faculty of Dentistry, Chulalongkorn University, Bangkok, Thailand

Address correspondence to: Dr Gerlig Widmann
E-mail: *gerlig.widmann@i-med.ac.at*

Objective: The aim of this study was to evaluate whether application of ultralow dose protocols and iterative reconstruction technology (IRT) influence quantitative Hounsfield units (HUs) and contrast-to-noise ratio (CNR) in dentomaxillofacial CT imaging.
Methods: A phantom with inserts of five types of materials was scanned using protocols for (a) a clinical reference for navigated surgery (CT dose index volume 36.58 mGy), (b) low-dose sinus imaging (18.28 mGy) and (c) four ultralow dose imaging (4.14, 2.63, 0.99 and 0.53 mGy). All images were reconstructed using: (i) filtered back projection (FBP); (ii) IRT: adaptive statistical iterative reconstruction-50 (ASIR-50), ASIR-100 and model-based iterative reconstruction (MBIR); and (iii) standard (std) and bone kernel. Mean HU, CNR and average HU error after recalibration were determined. Each combination of protocols was compared using Friedman analysis of variance, followed by Dunn's multiple comparison test.
Results: Pearson's sample correlation coefficients were all >0.99. Ultralow dose protocols using FBP showed errors of up to 273 HU. Std kernels had less HU variability than bone kernels. MBIR reduced the error value for the lowest dose protocol to 138 HU and retained the highest relative CNR. ASIR could not demonstrate significant advantages over FBP.
Conclusions: Considering a potential dose reduction as low as 1.5% of a std protocol, ultralow dose protocols and IRT should be further tested for clinical dentomaxillofacial CT imaging.
Advances in knowledge: HU as a surrogate for bone density may vary significantly in CT ultralow dose imaging. However, use of std kernels and MBIR technology reduce HU error values and may retain the highest CNR.

INTRODUCTION

In addition to dimensional analysis, radiological estimation of bone quality is an essential element of pre-surgical implant planning. Calculation of densities based on Gray values obtained from CT scans has become easily applicable and correlates well with fastening torque and implant stability values.[1] In CT, Gray values can be calibrated as Hounsfield units (HUs), which are defined as linear transformations of measured X-ray attenuation coefficients of materials with reference to water.[2] The HU scale is based on two fixed values, which are 0 HU for water and −1000 HU for air.

In the past years, cone beam CT (CBCT) has been increasingly overtaking CT in dentomaxillofacial imaging. CBCT scanners can be installed in dental practices and are argued to be a low-dose modality compared with MSCT. However, several important misconceptions have to be cleared. Owing to various reasons inherent to the CBCT technique, such as limited field size, relatively high amount of scattered radiation, limitations of currently applied reconstruction algorithms and asymmetrical patient positioning, quantitative use of CBCT Gray value-based density measures cannot be recommended.[2,3] Second, CBCT shows a wide range in doses, overlapping with doses from CT and panoramic radiography, depending on field of view, imaging parameter and manufacturer.[4–6]

It is not commonly known that recent CT technology allows high-resolution protocols at dose exposition equal or lower than CBCT (= ultralow dose CT).[7,8] To reduce the increase of noise in ultralow dose imaging, iterative

reconstruction technologies (IRTs) such as adaptive statistical iterative reconstruction (ASIR) and model-based iterative reconstruction (MBIR) have been implemented with promising potential.[8,9] To the best of the authors' knowledge, this is the first study that aimed to evaluate whether application of ultralow dose protocols and IRT influence HU and contrast-to-noise ratio (CNR), with a specific focus on dentomaxillofacial CT imaging.

METHODS AND MATERIALS

SedentexCT phantom and inserts

A customized polymethyl methacrylate (PMMA) phantom (Leeds Test Objects Ltd., Boroughbridge, UK) was used. The phantom is cylindrical and represents an adult head (diameter 16.0 cm, height 17.7 cm). It contains one central and six peripheral holes, which allow for the placement of inserts for image quality analysis. In this study, six different inserts were used. They consisted of small PMMA cylinders (diameter 3.5 cm, height 2.0 cm) containing a central rod of 1.0 cm diameter. Five types of materials were used for the central rod: air, aluminium and hydroxyapatite (HA) in three different concentrations (50, 100 and 200 mg cm^{-3}). The three HA test materials represent the bone. The sixth insert contained homogeneous PMMA. As the region of interest (ROI) for dental radiographic images is typically located close to the periphery of the head, the inserts were placed in the six peripheral columns of the large phantom. The rest of the phantom was filled up using PMMA inserts to ensure that the total mass of an average human head was represented. More details of the phantom including images can be found in Pauwels et al.[10]

CT scanning

The entire phantom was scanned using the 64-multislice CT scanner Discovery™ CT750 HD (GE Healthcare, Vienna, Austria). This scanner is regularly used for surgical planning in guided implant and maxillofacial surgery. The following high-resolution protocols were used: (a) a reference protocol for navigated dental surgery, (b) a low-dose sinusitis protocol and (c) a series of four ultralow dose protocols (I–IV) (Figure 1, Table 1). All protocols used fixed tube potential and mA levels without dose modulation, collimation 20 × 0.625 mm, pitch 0.5, slice thickness 0.625 mm and reconstructive increment 0.625 mm. CT dose index volume ($CTDI_{vol}$) values for the reference, sinusitis and ultralow dose I–IV protocols were 36.58, 18.28, 4.14, 2.63, 0.99 and 0.53 mGy, respectively. All images were reconstructed using standard (std) filtered back projection (FBP) and the following IRTs: ASIR-50 (50% FBP, 50% ASIR), ASIR-100 (0% FBP, 100% ASIR) and MBIR. ASIR uses information obtained from the FBP algorithm but integrates a comparison of the pixel values with an ideal value to selectively identify and then subtract noise from an image at adaptive blend levels.[9] MBIR does not rely on the FBP as a starting point but instead uses a more complex system of prediction models, including noise and the spatial and geometric features of the X-ray beam and detector technology.[11] Std and bone kernels were used in all protocols and reconstructions except MBIR, for which only the std kernel was available (Figure 2, Table 1).

All images were exported in digital imaging and communications in medicine format into IMPAX EE (Agfa HealthCare, Bonn, Germany) picture archiving and communication system for image analysis.

Image analysis

Hounsfield units

For all six materials inside the inserts, the mean HU was obtained using a circular ROI of 47 mm^2. The ROI included

Figure 1. Influence of exposure (protocol): images of test body, hydroxyapatite at a concentration of 200 mg cm^{-3} using reference, sinusitis and ultralow dose I–IV protocols. All images use filtered back projection and standard kernel. Note the increase of noise for continuous dose reduction.

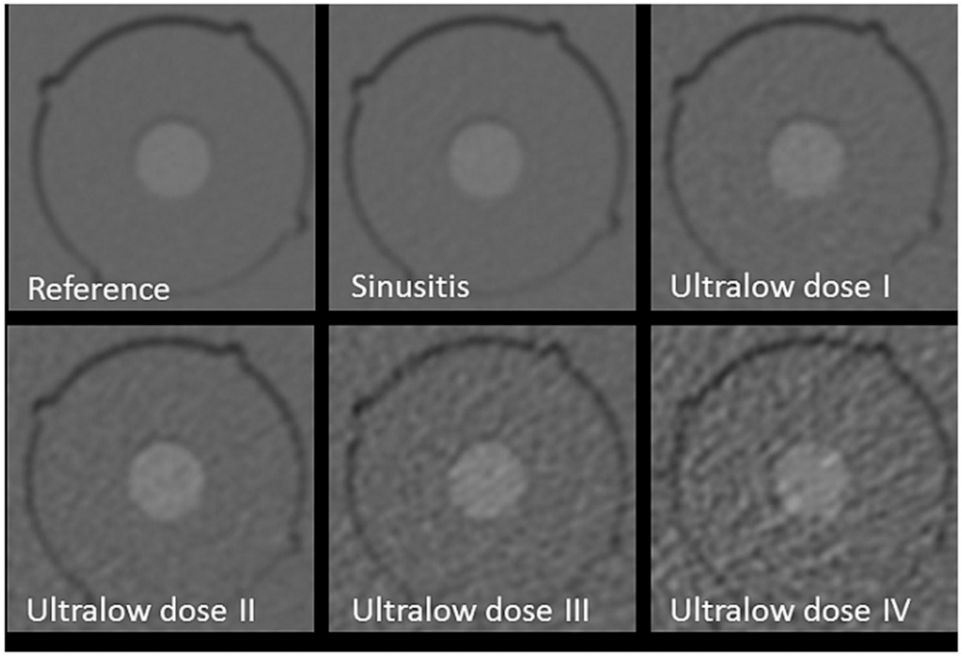

Table 1. List of exposure parameters and reconstruction techniques used to produce the various combinations of MSCT image datasets

Exposure (protocol)	Reconstruction technique	Kernel	kV	mAs	Rotation time (s)	$CTDI_{vol}$ (mGy)	DLP (mGy cm)
Reference	FBP	bone, std	120	100	1	36.58	808.86
	ASIR-50	bone, std					
	ASIR-100	bone, std					
	MBIR	std					
Sinusitis	FBP	bone, std	120	50	1	18.28	403.18
	ASIR-50	bone, std					
	ASIR-100	bone, std					
	MBIR						
Ultralow dose I	FBP	bone, std	100	35	0.5	4.14	92.04
	ASIR-50	bone, std					
	ASIR-100	bone, std					
	MBIR	std					
Ultralow dose II	FBP	bone, std	80	40	0.5	2.63	58.05
	ASIR-50	bone, std					
	ASIR-100	bone, std					
	MBIR	std					
Ultralow dose III	FBP	bone, std	80	15	0.5	0.99	21.77
	ASIR-50	bone, std					
	ASIR-100	bone, std					
	MBIR	std					
Ultralow dose IV	FBP	bone, std	80	10	0.4	0.53	11.59
	ASIR-50	bone, std					
	ASIR-100	bone, std					
	MBIR	std					

ASIR, adaptive statistical iterative reconstruction; $CTDI_{vol}$, CT dose index volume; DLP, dose–length product; FBP, filtered back projection; kV, tube potential; MBIR, model-based iterative reconstruction; std, standard.

most of the test material but excluded the margin to avoid errors from calculating HU in the surrounding PMAA. Measurements from ten consecutive axial slices were averaged, leading to a total measurement area of 470 mm^2.

Contrast noise ratio

The CNR for each material m was calculated using the following formula:

$$CNR_m = \frac{|MHU_m - MHU_{PMMA}|}{\sqrt{(SD_m^2 + SD_{PMMA}^2)}}$$

with MHU, the mean HU value, and SD, the std deviation of HU, averaged over ten axial slices.

Statistical analysis

HU of different protocols were statistically compared because the data were not normally distributed; Dunn's multiple comparison test was used to compare each combination of protocols ($\alpha = 0.05$).

Additional analysis of HU stability was performed according to the analysis method used in Pauwels et al,[12] Pearson's sample correlation coefficient was calculated for all six materials (r_{ALL}) and for the four medium-density materials only (r_{MED}). In addition, for each protocol, HU were recalibrated using the values for *air* and aluminium (*alu*) for a calibration protocol. Calibration protocols for this analysis differed depending on the purpose of the comparison and are detailed below. The "error" after recalibration for the four remaining materials m, *i.e.* the difference between the recalibrated value for that protocol p and the measured value for the calibration protocol c, was calculated as:

Figure 2. Influence of reconstruction and kernel: images of test body, hydroxyapatite at a concentration of 200 mg cm^{-3} using protocol ultralow dose IV and filtered back projection (FBP), adaptive statistical iterative reconstruction (ASIR)-50, ASIR-100 and model-based iterative reconstruction (MBIR) showing corresponding standard (std) kernel on the left and bone kernel on the right. Note the decrease of noise for increased level of iterative reconstruction and std *vs* bone kernel.

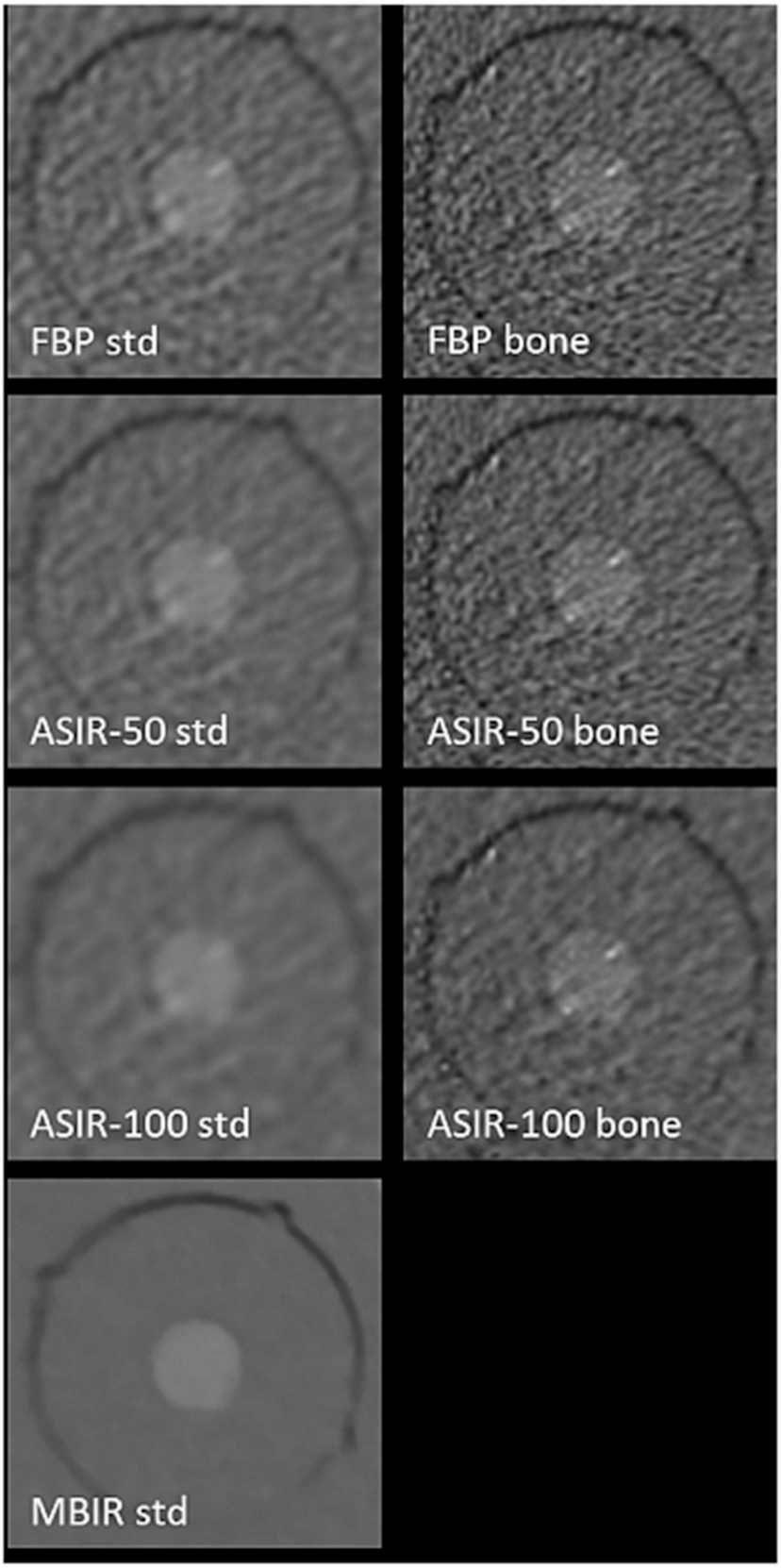

$$Error_m = \left| \left(MHU_{p,m} MHU_{p,air}\right) \left(\frac{MHU_{c,alu} MHU_{c,air}}{MHU_{p,alu} MHU_{p,air}}\right) - \left(MHU_{c,m} MHU_{c,air}\right) \right|$$

The error values for the four materials under consideration (*i.e.* PMMA and HA 50, HA 100, HA 200 mg cm^{-3}) were then averaged.

Effect of exposure (protocol)

Every image was compared with the corresponding "reference" protocol (*i.e.* with different exposure parameters but the same reconstruction technique and kernel). Thus, for each non-reference protocol, the corresponding reference protocol acted as calibration protocol for the error estimation.

Effect of reconstruction

Every image was compared with the FBP image for the same protocol and kernel (*i.e.* exposure parameters are fixed and bone/std is fixed). Thus, for each non-FBP protocol, the corresponding FBP protocol acted as the calibration protocol for the error estimation.

Effect of kernel

Every "bone" image was compared with the corresponding "std" image (*i.e.* exposure parameters and reconstruction technique are fixed). Thus, for each bone protocol, the corresponding std protocol acted as the calibration protocol for the error estimation.

RESULTS

HU analysis

Out of 231 pairwise comparisons made between exposure protocols, 120 (52%) showed significantly different HUs ($p < 0.05$) (Tables 2 and 3). Average correlation coefficients were: between exposure protocols: r_{ALL} = 0.9970, r_{MED} = 0.9981; between reconstruction algorithms: r_{ALL} = 1.0000, r_{MED} = 0.9995; and between std and bone kernels: r_{ALL} = 0.9994, r_{MED} = 0.9954. Although correlation was high throughout due to the nature of the data (*i.e.* the inherent correlation between material density and Gray values in CT), it could thus be seen that the use of a different exposure affected HU stability more than the use of a different reconstruction algorithm and that the use of a std or bone kernel affected HU in the medium density range. The average error values showing the effect of protocol (=exposure), reconstruction and convolution kernel are found in Table 4.

Effect of exposure (protocol)

Reference *vs* sinusitis showed no significant differences for any reconstruction technique. Ultralow doses I–III showed significant differences *vs* reference and sinusitis in most cases (28/42 pairwise comparisons, or 23/28 for ultralow dose II–III only). Interestingly, ultralow dose IV was not significant *vs* reference or sinusitis in most cases (9/14 comparisons). MBIR showed the highest stability for changing exposure parameters (4/15 comparisons significant), ASIR 100 (bone) the lowest (11/15 comparisons significant) (Table 2).

The error values (rounded up to 0 decimals) showed hardly any effect of sinusitis protocol *vs* reference protocol, with error values of 2–11 HU. Ultralow dose protocols showed relatively large differences with error values of 67–108 HU for ultralow dose Protocol I, 173–186 HU for ultralow dose Protocol II, 162–201 HU for ultralow dose Protocol III and 138–273 HU for ultralow dose Protocol IV (Table 4).

Effect of reconstruction

FBP vs ASIR showed no significant differences in almost all cases (35/36 comparisons). For comparisons of MBIR *vs* FBP/ASIR, mixed results were found (50% of comparisons significant) (Table 3).

In terms of HU error after calibration, reconstruction technique had little effect (error mostly ≤10 HU, ranging between 2 and 35 HU), with MIBR showing the largest effect overall (8–32 HU). Ultralow dose Protocol IV showed the largest effect of reconstruction technique with error values of 11–35 HU (Table 4).

Effect of kernel

When comparing std *vs* bone kernel for corresponding protocols, significant differences were found in the majority of cases (15/18 comparisons) (see Table 3).

Table 2. Effect of exposure (protocol)

Exposure protocol	Reference	Sinusitis	Ultralow dose I	Ultralow dose II	Ultralow dose III	Ultralow dose IV
Reference	–	0	3	6	7	4
Sinusitis	0	–	2	4	6	5
Ultralow dose I	3	2	–	0	3	6
Ultralow dose II	6	4	0	–	0	5
Ultralow dose III	7	6	3	0	–	4
Ultralow dose IV	4	5	6	5	4	–

Comparison of Gray values for six scanned materials using Dunn's multiple comparison test.
For each pair of exposure protocols, pairwise comparisons were made for each reconstruction technique ($n = 7$).
The total number of significant comparisons ($\alpha = 0.05$), out of seven, are shown.

Table 3. Effect of reconstruction technique and kernel

Reconstruction technique (kernel)	Significant	Not significant
FBP (std) *vs* ASIR-50 (std)	0	6
FBP (std) *vs* ASIR-100 (std)	0	6
FBP (std) *vs* MBIR (std)	4	2
FBP (std) *vs* FBP (bone)	6	0
FBP (std) *vs* ASIR-50 (bone)	5	1
FBP (std) *vs* ASIR-100 (bone)	4	2
ASIR-50 (std) *vs* ASIR-100 (std)	0	6
ASIR-50 (std) *vs* MBIR (std)	2	4
ASIR-50 (std) *vs* FBP (bone)	6	0
ASIR-50 (std) *vs* ASIR-50 (bone)	5	1
ASIR-50 (std) *vs* ASIR-100 (bone)	4	2
ASIR-100 (std) *vs* MBIR (std)	3	3
ASIR-100 (std) *vs* FBP (bone)	6	0
ASIR-100 (std) *vs* ASIR-50 (bone)	6	0
ASIR-100 (std) *vs* ASIR-100 (bone)	4	2
MBIR (std) *vs* FBP (bone)	3	3
MBIR (std) *vs* ASIR-50 (bone)	3	3
MBIR (std) *vs* ASIR-100 (bone)	3	3
FBP (bone) *vs* ASIR-50 (bone)	0	6
FBP (bone) *vs* ASIR-100 (bone)	1	5
ASIR-50 (bone) vs ASIR-100 (bone)	0	6

ASIR, adaptive statistical iterative reconstruction; FBP, filtered back projection; MBIR, model-based iterative reconstruction; std, standard.
Comparison of Gray values for six scanned materials using Dunn's multiple comparison test.
For each pair of reconstructions, pairwise comparisons were made for each exposure protocol ($n = 6$).
The total number of significant and non-significant comparisons ($\alpha = 0.05$) are shown.

Considering the error values, there was hardly any effect of convolution kernel for reference and sinusitis protocols (error 3–7 HU). Larger effects were seen for low-dose protocols with 19–34 HU for ultralow dose Protocols I, II and III, and 77–108 HU for ultralow dose Protocol IV (Table 4). In ultralow dose Protocol IV, the bone kernel showed a dramatic influence on Gray values for all materials except air and aluminium: mean HU using bone *vs* std kernel for low dose Protocol IV were −5 to −1 *vs* 124–149 HU for HA 50 mg cm^{-3}; 84–97 *vs* 221–253 HU for HA 100 mg cm^{-3}; 296–304 *vs* 448–506 HU for material HA 200 mg cm^{-3}; and −271 to −244 *vs* 78–123 HU for PMMA.

Contrast-to-noise ratio

The CNR results are given in Table 5. The sinusitis protocol generally showed a lower CNR than the reference protocol (−12%), and ultralow dose Protocols I–IV showed progressively lower CNRs, with an average decrease in CNR of 45%, 48%, 61% and 69%, respectively (Table 2, Figure 1). When comparing the reconstruction techniques, MIBR has the highest CNR throughout, followed by ASIR 100 (std), ASIR 50 (std), FBP (std), ASIR 100 (bone), ASIR 50 (bone) and FBP (bone). Std kernels showed higher CNR than bone kernels throughout (Table 2, Figure 2).

DISCUSSION

The increased use of CT and CBCT imaging in the dentomaxillofacial[13] field raised serious concerns of radiation exposure. Legislative authorities and radiologic societies drive guidelines for evidence-based use of CT/CBCT imaging and intend to reduce radiation exposition to "as low as reasonably achievable" levels[14]. However, the as low as reasonably achievable levels depend on technological features and on the ability to sufficiently answer the indicated clinical questions. Modern CT technology has remarkable means for dose reduction such as 64-row multislice scanning and above, automatic exposure control, optimization of tube potential, beam-shaping filters, dynamic *z*-axis beam collimation and IRTs.[15] Fortunately, dentomaxillofacial imaging focuses on tissues with high anatomical contrast (*e.g.* bone, teeth), which are very suitable for dose reduction. Compared with a reference protocol at a $CTDI_{vol}$ of 35.3 mGy, the use of protocols with a $CTDI_{vol}$ of 1.0 and 2.6 mGy may be sufficient for the diagnosis of dislocated and non-dislocated craniofacial fractures, respectively.[7] Compared

Table 4. Error values (HU), after recalculation of HU values *vs* a calibration protocol, showing effect of exposure, reconstruction and convolution kernel

Protocol	Reconstruction	Std/bone	Effect of exposure[a]	Effect of reconstruction[b]	Effect of kernel[c]
Reference	FBP	Std			
	ASIR-50			10.18	
	ASIR-100			5.98	
	MBIR			18.40	
	FBP	Bone			4.41
	ASIR-50			3.61	6.34
	ASIR-100			3.26	3.14
Sinusitis	FBP	Std	4.22		
	ASIR-50		6.16	2.06	
	ASIR-100		2.34	3.94	
	MBIR		3.78	11.05	
	FBP	Bone	10.66		7.13
	ASIR-50		4.73	2.84	3.60
	ASIR-100		3.44	6.99	5.89
Low dose I	FBP	Std	75.47		
	ASIR-50		74.42	10.62	
	ASIR-100		81.54	12.06	
	MBIR		66.51	9.21	
	FBP	Bone	107.54		33.51
	ASIR-50		103.26	3.82	22.14
	ASIR-100		101.58	5.58	18.62
Low dose II	FBP	Std	185.74		
	ASIR-50		176.89	10.60	
	ASIR-100		177.75	6.60	
	MBIR		163.07	7.67	
	FBP	Bone	182.52		11.22
	ASIR-50		178.82	7.64	16.37
	ASIR-100		172.61	7.90	17.30
Low dose III	FBP	Std	185.98		
	ASIR-50		174.62	6.33	
	ASIR-100		187.40	7.27	
	MBIR		162.26	9.03	
	FBP	Bone	201.32		26.76
	ASIR-50		196.65	3.38	30.36
	ASIR-100		189.11	10.19	25.93

(Continued)

Table 4. (Continued)

Protocol	Reconstruction	Std/bone	Effect of exposure[a]	Effect of reconstruction[b]	Effect of kernel[c]
Low dose IV	FBP	Std	181.47		
	ASIR-50		173.94	10.95	
	ASIR-100		178.58	10.97	
	MBIR		138.28	32.44	
	FBP	Bone	272.67		107.82
	ASIR-50		258.61	10.76	90.00
	ASIR-100		234.87	35.27	76.95

ASIR, adaptive statistical iterative reconstruction; FBP, filtered back projection; MBIR, model-based iterative reconstruction; std, standard.
[a]For each non-Reference protocol, the corresponding Reference protocol acted as calibration protocol for the error estimation.
[b]For each non-FBP protocol, the corresponding FBP protocol acted as calibration protocol for the error estimation.
[c]For each bone protocol, the corresponding 'std' protocol acted as calibration protocol for the error estimation.

with the std image reconstruction technique of FBP, additional application of IRTs in substantially reduced image noise and improved subjective quality of low dose images. In a prior study, two-dimensional images using ASIR-100 at $CTDI_{vol}$ of 3.48 mGy, ASIR-100 at $CTDI_{vol}$ of 2.19 mGy and MBIR at $CTDI_{vol}$ of 0.82 mGy; and three-dimensional images using MBIR at $CTDI_{vol}$ of 0.22 mGy showed no significant difference in subjective image quality, as compared with a FBP reference at $CTDI_{vol}$ of 30.48 mGy.[8]

In the present study, a low-dose sinusitis protocol at $CTDI_{vol}$ of 18.28 mGy and several ultralow dose protocols at $CTDI_{vol}$ 4.14, 2.63, 0.99 and 0.53 mGy were evaluated in terms of HU stability and CNR. Compared with the reference protocol at $CTDI_{vol}$ of 36.58 mGy, the low-dose sinusitis protocol had a radiation exposure of only 50%, and the subsequent ultralow dose protocols I–IV have exposures of 11%, 7%, 3% and 1.5%, respectively. Following the method of Dixon and Boone,[13] Kyriakou et al[16] reported comparable dose levels of a CT protocol at $CTDI_w$ of 2.7 mGy, and four different CBCT with $CTDI_w$ of 2.3–3.1 mGy. Dose reduction in the present study was well below these values and, important to note, may even be lower than that of most dentomaxillofacial CBCT devices.[5,6]

As extensively discussed in the literature, CBCT may currently not be reliable for quantitative bone density measures.[2,3,17,18] By contrast, CT-based measures using HU are relatively consistent across different CT scanners and an integrated part of quality control. In 2001, Norton and Gamble[19] published quantitative ranges of HU values for the Lekholm and Zarb classification (1985), with >+850 HU for Quality 1 (almost the entire jaw is composed of homogeneous bone; ROI, anterior mandible), +500 to +850 for Quality 2/3 [a thick layer (2) or thin layer (3) of cortical bone surrounds a core of dense trabecular bone; ROI, posterior mandible or anterior maxilla], <0 to +500 for Quality 4 (a thin layer of cortical bone surrounds a core of low-density trabecular bone; ROI, posterior maxilla or tuberosity region). However, the authors used "std dose" protocols, and it is unclear whether HU measures remain stable with the currently available ultralow dose technology and IRTs.

In the present study, a customized phantom[20] was used, which was developed as a quality control phantom for CBCT scanners and previously applied for comparison of the variability of dentomaxillofacial CBCT Gray values comparing a large number of CBCT scanners and protocols with a 64-slice CT scanner.[12] Most CBCT scanners showed a good overall correlation with MSCT, with Pearson correlation coefficients ranging between 0.7014 and 0.9996 in the full-density range (r_{ALL}) and between 0.5620 and 0.9991 in the medium-density range (r_{MED}). However, large error values (typically between 50 and 200 Gray values, but ranging up to 1562 Gray values) were observed, predominately related to the large amount of scatter, effects related to the limited field of view size and histogram shifts.[12] The Pearson correlation coefficients in the present study were all well above 0.99. HU were very stable for air and aluminium, but for the bone-equivalent test materials, there may be a relevant variability. Although there was hardly any difference between the low-dose sinusitis and the reference protocol, considerable error values were found for the ultralow dose protocols, with lower doses leading to higher error values. Thus, at the very end of dose reduction, differentiation between highly dense (>850 HU), dense (+500 to +850 HU) and low-density trabecular bone (<0 to +500 HU) may become less clear. MBIR demonstrated the lowest error values in all ultralow dose protocols and showed a mean error of 138 HU for ultralow dose Protocol IV. For this protocol, the largest effect of reconstruction technique was seen. In addition, reconstruction kernel may play an essential role, as in ultralow dose Protocol IV, a dramatic influence on HU values for test materials was seen.

Reduction in dose increased noise and thus reduced CNR. As expected, std kernel showed a significantly higher CNR than bone kernel. The advantage of a higher CNR using std kernel goes along with drawbacks in spatial resolution. Bone kernels outline thin bone contours and trabecular bone structure but at the cost of increased noise. MIBR demonstrated the highest CNR throughout, followed by ASIR 100, ASIR 50 and FBP. MBIR was able to retain the highest relative CNR at the lowest dose and showed a approximately 55% reduction in CNR for ultralow dose IV *vs* reference protocols, whereas the FBP std

Table 5. Contrast-to-noise ratios (CNRs) of all protocols, reconstructions and convolution kernels [standard (std)/bone]

Protocol	Reconstruction	Kernel	CNR, air	CNR, aluminium	CNR, HA 50	CNR, HA 100	CNR, HA 200
Reference	FBP	std	41.04	28.60	0.65	3.81	9.74
	ASIR-50		51.96	38.08	0.66	5.11	13.43
	ASIR-100		57.63	64.24	0.78	6.78	15.89
	MBIR		79.97	103.04	1.26	7.48	21.62
	FBP	bone	17.48	26.46	0.17	1.08	3.51
	ASIR-50		20.77	32.69	0.29	1.48	4.44
	ASIR-100		31.72	43.41	0.44	2.23	6.46
Sinusitis	FBP	std	33.37	36.70	0.38	2.39	7.39
	ASIR-50		48.20	55.29	0.64	3.22	9.72
	ASIR-100		63.22	68.25	0.90	4.60	11.48
	MBIR		73.47	80.78	1.00	4.80	12.89
	FBP	bone	12.34	20.68	0.17	0.89	2.66
	ASIR-50		14.01	22.78	0.16	0.94	2.92
	ASIR-100		22.71	28.32	0.18	1.64	4.72
Ultralow dose I	FBP	std	15.85	19.85	0.37	1.40	3.77
	ASIR-50		20.73	29.61	0.34	2.03	5.33
	ASIR-100		29.30	41.69	0.64	3.06	7.44
	MBIR		53.88	81.86	1.11	5.24	14.76
	FBP	bone	6.06	11.26	0.08	0.51	1.52
	ASIR-50		6.77	12.19	0.04	0.58	1.69
	ASIR-100		10.37	16.37	0.03	0.82	2.30
Ultralow dose II	FBP	std	10.89	19.37	0.31	1.52	3.58
	ASIR-50		15.77	29.30	0.73	2.03	5.09
	ASIR-100		25.70	45.38	0.82	3.19	8.36
	MBIR		47.90	79.28	1.56	5.90	17.30
	FBP	bone	4.20	10.17	0.01	0.47	1.27
	ASIR-50		4.99	12.28	0.09	0.54	1.57
	ASIR-100		8.10	19.02	0.04	0.89	2.46
Ultralow dose III	FBP	std	7.29	16.98	0.26	0.90	2.34
	ASIR-50		10.36	23.42	0.24	1.14	3.24
	ASIR-100		14.09	34.08	0.51	1.72	4.72
	MBIR		36.39	70.27	1.44	4.82	12.62
	FBP	bone	2.43	6.20	0.14	0.44	0.92
	ASIR-50		2.94	7.15	0.16	0.50	1.10
	ASIR-100		5.36	10.59	0.31	0.84	1.81

(Continued)

Table 5. (Continued)

Protocol	Reconstruction	Kernel	CNR, air	CNR, aluminium	CNR, HA 50	CNR, HA 100	CNR, HA 200
Ultralow dose IV	FBP	std	5.18	13.87	0.17	0.62	1.65
	ASIR-50		6.77	17.74	0.15	0.71	2.08
	ASIR-100		10.05	26.68	0.11	1.17	2.96
	MBIR		35.69	56.67	1.67	4.95	11.08
	FBP	bone	1.31	4.10	0.41	0.55	0.88
	ASIR-50		1.49	4.58	0.48	0.64	1.00
	ASIR-100		2.19	6.12	0.78	1.07	1.52

ASIR, adaptive statistical iterative reconstruction; FBP, filtered back projection; HA, hydroxyapatite; MBIR, model-based iterative reconstruction.

kernel showed a 87% reduction. Interestingly, ASIR could not demonstrate significant advantages over FBP in terms of CNR.

This study was performed using a phantom that included inserts with mean HU for HA 50, HA 100 and HA 200; and PMAA of 132.3, 202.9 and 365.8; and 117.5 (reference protocol, FBP and std kernel). These values were within the range of bone Quality 4 according to Norton and Gamble.[19] Test material for reference values of bone Quality 1 and 2/3 was not available; however, similar HU stability can be expected at density ranges corresponding to these bone quality groups. The diagnostic CT scanner is regularly calibrated for accuracy and uniformity of HU based on a scanner driven quality control procedure using a tube potential spectrum ranging from 80 to 140 kV. However, direct comparisons of ultralow dose HU (with extreme low levels of mA) to previous studies on HU-based classification of bone density may be problematic. To evaluate potential (mis) classification of bone quality, the outcome of this study may need to be verified in a study using a series of human jaw bone specimens with distinct bone density. The ultimate test would be an observer study assessing the impact of reduced dose on diagnostic accuracy.

CONCLUSION

Ultralow dose protocols with exposures of only 11%, 7%, 3% and 1.5% of a high-resolution reference protocol were tested for variability of HU and CNR. Dose reduction influenced HU. Std kernels effectively reduced the variability of HU and should be provided in addition to bone kernels. MBIR with std kernel had the most beneficial effect on HU. In addition, MBIR improved CNR of ultralow dose images and may therefore be recommended as an additional reconstruction technique. By contrast, ASIR could not demonstrate significant advantages over FBP. Owing to the substantial reduction of radiation dose, it is strongly recommended to test ultralow dose protocols and MBIR in further clinical studies on dentomaxillofacial imaging applications.

ACKNOWLEDGMENTS

The authors thank Michael Steurer, MSc, BSc, for his help during executing the CT scans.

REFERENCES

1. Turkyilmaz I, Tumer C, Ozbek EN, Tözüm TF. Relations between the bone density values from computerized tomography, and implant stability parameters: a clinical study of 230 regular platform implants. *J Clin Periodontol* 2007; **34**: 716–22. doi: http://dx.doi.org/10.1111/j.1600-051X.2007.01112.x
2. Pauwels R, Jacobs R, Singer SR, Mupparapu M. CBCT-based bone quality assessment: are Hounsfield units applicable? *Dentomaxillofac Radiol* 2015; **44**: 20140238. doi: http://dx.doi.org/10.1259/dmfr.20140238
3. Nackaerts O, Maes F, Yan H, Couto Souza P, Pauwels R, Jacobs R. Analysis of intensity variability in multislice and cone beam computed tomography. *Clin Oral Implants Research* 2011; **22**: 873–9. doi: http://dx.doi.org/10.1111/j.1600-0501.2010.02076.x
4. Pauwels R. Cone beam CT for dental and maxillofacial imaging: dose matters. *Radiat Prot Dosimetry* 2015; **165**: 156–61. doi: http://dx.doi.org/10.1093/rpd/ncv057
5. Pauwels R, Beinsberger J, Collaert B, Theodorakou C, Rogers J, Walker A, et al; SEDENTEXCT Project Consortium. Effective dose range for dental cone beam computed tomography scanners. *Eur J Radiol* 2012; **81**: 267–71. doi: http://dx.doi.org/10.1016/j.ejrad.2010.11.028
6. Bornstein MM, Scarfe WC, Vaughn VM, Jacobs R. Cone beam computed tomography in implant dentistry: a systematic review focusing on guidelines, indications, and radiation dose risks. *Int J Oral Maxillofac Implants* 2014; **29**: 55–77. doi: http://dx.doi.org/10.11607/jomi.2014suppl.g1.4
7. Widmann G, Dalla Torre D, Hoermann R, Schullian P, Gassner EM, Bale R, et al. Ultralow-dose computed tomography imaging for surgery of midfacial and orbital fractures using ASIR and MBIR. *Int J Oral Maxillofac Surg* 2015; **44**: 441–6. doi: http://dx.doi.org/10.1016/j.ijom.2015.01.011
8. Widmann G, Fasser M, Schullian P, Zangerl A, Puelacher W, Kral F, et al. Substantial dose reduction in modern multi-slice spiral computed tomography (MSCT)-guided craniofacial and skull base surgery. *Rofo* 2012; **184**: 136–42. doi: http://dx.doi.org/10.1055/s-0031-1281971
9. Silva AC, Lawder HJ, Hara A, Kujak J, Pavlicek W. Innovations in CT dose reduction strategy: application of the adaptive statistical iterative reconstruction algorithm.

AJR Am J Roentgenol 2010; **194**: 191–9. doi: http://dx.doi.org/10.2214/AJR.09.2953

10. Pauwels R, Stamatakis H, Manousaridis G, Walker A, Michielsen K, Bosmans H, et al; SEDENTEXCT Project Consortium. Development and applicability of a quality control phantom for dental cone-beam CT. *J Appl Clin Med Phys* 2011; **12**: 3478. doi: http://dx.doi.org/10.1120/jacmp.v12i4.3478
11. Fleischmann D, Boas FE. Computed tomography–old ideas and new technology. *Eur Radiol* 2011; **21**: 510–7. doi: http://dx.doi.org/10.1007/s00330-011-2056-z
12. Pauwels R, Nackaerts O, Bellaiche N, Stamatakis H, Tsiklakis K, Walker A, et al; SEDENTEXCT Project Consortium. Variability of dental cone beam CT grey values for density estimations. *Br J Radiol* 2013; **86**: 20120135. doi: http://dx.doi.org/10.1259/bjr.20120135
13. Dixon RL, Boone JM. Cone beam CT dosimetry: a unified and self-consistent approach including all scan modalities–with or without phantom motion. *Med Phys* 2010; **37**: 2703–18. doi: http://dx.doi.org/10.1118/1.3395578
14. Kalra MK, Sodickson AD, Mayo-Smith WW. CT Radiation: key concepts for gentle and wise use. *Radiographics* 2015; **35**: 1706–21. doi: http://dx.doi.org/10.1148/rg.2015150118
15. McCollough CH, Chen GH, Kalender W, Leng S, Samei E, Taguchi K, et al. Achieving routine submillisievert CT scanning: report from the summit on management of radiation dose in CT. *Radiology* 2012; **264**: 567–80. doi: http://dx.doi.org/10.1148/radiol.12112265
16. Kyriakou Y, Kolditz D, Langner O, Krause J, Kalender W. Digital volume tomography (DVT) and multislice spiral CT (MSCT): an objective examination of dose and image quality [. In German.] *Rofo* 2011; **183**: 144–53. doi: http://dx.doi.org/10.1055/s-0029-1245709
17. Nackaerts O, Depypere M, Zhang G, Vandenberghe B, Maes F, Jacobs R; SEDENTEXCT Project Consortium. Segmentation of trabecular jaw bone on cone beam CT datasets. *Clin Implant Dent Relat Res.* 2015; **17**: 1082–91. doi: http://dx.doi.org/10.1111/cid.12217
18. Van Dessel J, Huang Y, Depypere M, Rubira-Bullen I, Maes F, Jacobs R. A comparative evaluation of cone beam CT and micro-CT on trabecular bone structures in the human mandible. *Dentomaxillofac Radiol* 2013; **42**: 20130145. doi: http://dx.doi.org/10.1259/dmfr.20130145
19. Norton MR, Gamble C. Bone classification: an objective scale of bone density using the computerized tomography scan. *Clin Oral Implants Res* 2001; **12**: 79–84. doi: http://dx.doi.org/10.1034/j.1600-0501.2001.012001079.x
20. Pauwels R, Beinsberger J, Stamatakis H, Tsiklakis K, Walker A, Bosmans H, et al; SEDENTEXCT Project Consortium. Comparison of spatial and contrast resolution for cone-beam computed tomography scanners. *Oral Surg Oral Med Oral Pathol Oral Radiol* 2012; **114**: 127–35. doi: http://dx.doi.org/10.1016/j.oooo.2012.01.020